Adaptive Control of Flexible Manipulators Carrying Large Uncertain Payloads

C. J. Damaren
Department of Mechanical Engineering
University of Canterbury
Private Bag 4800
Christchurch, New Zealand
e-mail: c.damaren@mech.canterbury.ac.nz

Received August 29, 1994; revised October 13, 1995; accepted November 2, 1995

An adaptive controller is presented for a manipulator with revolute joints and structurally flexible links which carries a rigid payload with unknown mass properties. Under the assumption that the payload mass is much greater than that of the manipulator, globally stable tracking of the Cartesian end-effector coordinates is established. Key ideas underlying the controller development are the passivity of a mapping involving the end-effector rates as part of the output and a fixed parameter feedforward which preserves this property. The concept of filtered error is borrowed from previous work on rigid arms and suitably modified in developing the adaptive law. Although measurements of the tip positions and rates are needed, there is no requirement for sensing of the elastic coordinates. A numerical example involving a six DOF manipulator with flexible links demonstrates excellent tracking with respect to a simulation based on the exact motion equations.

未知の質量の物体を載せる固定ペイロードを持ち上げる、回転ジョイントと柔軟構造リンクを持ったマニピュレータに対する、適応型コントローラについて説明する。ペイロードの質量がマニピュレータの質量と比較して非常に大きいと仮定すると、カルテシアン・エンドエフェクタ座標系におけるグローバルに安定したトラッキングが得られる。今回の研究で中心となるのは、エンドエフェクタ比を出力の一部とし含むマッピングの受動性と、この特性を保つための固定されたパラメータ・フィードフォアードに基づいたコントローラの開発である。フィルター誤差の概念は、既存の固定アームに関する研究から流用し、適応制御則の開発において適切に変更されている。先端部位置と比率の測定は必要であるが、弾性座標系でのセンシングは必要としない。フレキシブル・リンクを持った6 D. O. F. のマニピュレータの数値的な例を使って、厳密な運動方程式に基づいたシミュレーションにおける優秀なトラッキング性能について示す。

Journal of Robotic Systems 13(4), 219–228 (1996)

CCC 0741-2223/96/040219-10

INTRODUCTION

The last decade has seen the development of adaptive controllers for rigid robot arms which provide globally stable tracking in the presence of parameter ignorance.[1,2] As pointed out by several authors,[3–5] the success of these controllers can be explained using a passive systems approach. In particular, the model-based feedforward portion of the controller preserves the inherent passivity of the torque-to-joint rate map in the error dynamics. The other essential property is the linear dependence of the feedforward on the unknown robot parameters.

The extension of the above methodologies to the case of flexible link manipulators is made difficult because the map from torques to end-effector rates is not passive. In fact, it exhibits the nonlinear form of the nonminimum-phase property, namely instability of the zero dynamics.[6] The torque-to-joint rate map remains passive, but the creation of a feedforward which preserves this property is difficult. Lanari and Wen[7] have had some success in this regard, although their result is limited to joint space tracking and requires sensing of the elastic coordinates. DeLuca and Siciliano[8] have also developed a joint space feedforward strategy based on inverse dynamics, but passivity properties were not claimed.

Researchers have been quite successful in extending adaptive controllers for rigid robots to the case of rigid robots with flexible joints.[9–11] These approaches rely on the inherent passivity of the dynamics relating motor torque to motor rate. Our work is philosophically similar to that of Spong[9] who used a perturbation approach in dealing with weak joint elasticity. Most of the adaptive controllers to date for flexible link arms have dealt with the single-link case. Yuan, Book, and Siciliano[12] applied model reference adaptive control methods to the end-point tracking problem. Feliu, Rattan, and Brown[13] used a combination of feedforward and feedback which gave good end-point tracking for a single link. Pham, Khalil, & Chevallereau[14] implemented a modification of the rigid algorithm of Slotine & Li[1] on a two-link flexible arm in an experimental setting. Good end-effector tracking was obtained by virtue of the joint angle behavior.

The motivation for the present work stems from the use of robot arms to manipulate large, potentially poorly defined payloads in the space environment. Such systems are characterized by low mass relative to the carried payloads and must be treated as flexible. We seek an adaptive controller which provides tracking of the end-effector trajectories under the assumption that the payload is much more massive than the manipulator.

Two important results previously obtained by the author[15,16] provide the foundation for the approach taken here. First, the mapping from end-effector forces (inverse transpose of the Jacobian times torques) to an output termed the μ-tip rate was shown to be passive under the large payload assumption. The μ-tip position is a nonlinear, multilink generalization of the reflected tip position introduced by Wang & Vidyasagar[17] for a single link. Also, a feedforward control torque depending only on the mass properties of the payload was shown to maintain the passivity property with respect to the μ-tip rate tracking errors. Hence, asymptotic tracking in the known-parameter case could be obtained using a strictly passive controller (PD law).

Motivated by the corresponding work in the rigid case, an adaptive extension of our previous results will be presented. In the rigid case, a key modification is the introduction of the filtered error which ensures that the position errors tend toward zero.[1] The corresponding filtered error is introduced here, and passivity is demonstrated when it is used in the feedforward part of the controller. The passivity theorem is then used to suggest the correct forms of the parameter adaptation law and the feedback portion of the controller. Globally stable tracking of the true tip positions and rates is established using a Lyapunov stability analysis. A numerical example employing a six degree of freedom (DOF) robot with flexible links will be used to demonstrate the tracking performance using a simulation based on the exact motion equations.

2. DYNAMICS OF FLEXIBLE MANIPULATORS WITH LARGE PAYLOADS

We consider a chain of rigid or flexible bodies denoted by $\{\mathcal{B}_0, \ldots, \mathcal{B}_{N+1}\}$. $\mathcal{B}_0$ is taken to be rigid and fixed; its body-fixed frame $\mathcal{F}_0$ represents an inertial reference frame. The last link, $\mathcal{B}_N$, is assumed to carry a large rigid payload, $\mathcal{B}_{N+1}$, which is cantilevered to the end-effector. Its body-fixed frame $\mathcal{F}_{N+1}$ locates the end-effector. Using clamped-free basis functions to discretize the elastic deflections of the links, the motion equations for the system can be written as[18,19]

$$M(\mathbf{q})\ddot{\mathbf{q}} + D\dot{\mathbf{q}} + K\mathbf{q} = B\boldsymbol{\tau}(t) + f_{\text{non}}(\mathbf{q}, \dot{\mathbf{q}}), \qquad \mathbf{q} \triangleq \text{col}\{\boldsymbol{\theta}, \mathbf{q}_e\} \quad (1)$$

Assuming single DOF revolute joints, the joint angles are $\boldsymbol{\theta} \triangleq \text{col}\{\theta_n(t)\}$, $n = 1 \cdots N$, and $\mathbf{q}_e(t)$ is the

totality of elastic coordinates describing the flexible deformations. The mass matrix is $M = M^T > \mathbf{O}$, $\tau(t)$ is a column of applied joint torques, and f_{non} are nonlinear inertial forces which are quadratic in $\dot{\mathbf{q}}$. The damping, stiffness, and input matrices can be further partitioned as $D = \text{diag}\{\mathbf{O}, D_{ee}\}$, and $K = \text{diag}\{\mathbf{O}, K_{ee}\}$, and $B^T = [\mathbf{1}\ \mathbf{O}]$. The matrices D_{ee} and K_{ee} are positive-definite; for simplicity it will be assumed that they are constant.

The forward kinematics are summarized by defining $\boldsymbol{\rho}(t) = \boldsymbol{\rho}(\boldsymbol{\theta}, \mathbf{q}_e)$ whose upper half consists of the position of $\mathcal{F}_{N+1}$ with respect to $\mathcal{F}_0$ (expressed in $\mathcal{F}_0$), and the bottom contains three integrable attitude coordinates which paramaterize the rotation matrix $\mathbf{C}_{N+1,0}(\boldsymbol{\theta}, \mathbf{q}_e)$. The μ-tip rate[15,16] is defined by

$$\dot{\boldsymbol{\rho}}_\mu \triangleq J_\theta \dot{\boldsymbol{\theta}} + \mu J_e \dot{\mathbf{q}}_e = \dot{\boldsymbol{\rho}} - (1-\mu) J_e(\boldsymbol{\theta}, \mathbf{q}_e)\dot{\mathbf{q}}_e \quad (2)$$

where μ is a real parameter. The matrix $J_\theta \triangleq \partial\boldsymbol{\rho}/\partial\boldsymbol{\theta}^T$ will be called the rigid Jacobian and $J_e \triangleq \partial\boldsymbol{\rho}/\partial\mathbf{q}_e^T$ is the elastic Jacobian. Hence, for $\mu = 1$, $\dot{\boldsymbol{\rho}}_\mu \equiv \dot{\boldsymbol{\rho}}$. In general, $\dot{\boldsymbol{\rho}}_\mu = \mu\dot{\boldsymbol{\rho}} + (1-\mu)J_\theta\dot{\boldsymbol{\theta}}$ and hence $\boldsymbol{\rho}_\mu \doteq \mu\boldsymbol{\rho} + (1-\mu)F(\boldsymbol{\theta})$ where F is the rigid forward kinematics map. This follows from the approximation $J_\theta(\boldsymbol{\theta}, \mathbf{q}_e) \doteq J_\theta(\boldsymbol{\theta}, \mathbf{0})$ which is the Jacobian of the corresponding rigid manipulator.

We shall also require the body-frame velocities of the payload. Let $\boldsymbol{v}_t \triangleq \text{col}\{\mathbf{v}_t, \boldsymbol{\omega}_t\}$ where $\mathbf{v}_t$ and $\boldsymbol{\omega}_t$ denote the absolute velocity and angular velocity of $\mathcal{B}_{N+1}$ but expressed in $\mathcal{F}_{N+1}$. Hence,

$$\begin{aligned} \boldsymbol{v}_t &= P_t(\boldsymbol{\rho})\dot{\boldsymbol{\rho}} = \hat{J}_\theta\dot{\boldsymbol{\theta}} + \hat{J}_e\dot{\mathbf{q}}_e, \\ P_t &= \text{diag}\{\mathbf{C}_{N+1,0}(\boldsymbol{\rho}), \mathbf{S}_{N+1,0}(\boldsymbol{\rho})\} \end{aligned} \quad (3)$$

where $\mathbf{S}_{N+1,0}$ is the configuration-dependent matrix mapping Euler rates into angular velocity (expressed in the body frame), $\hat{J}_\theta \triangleq P_t J_\theta$, and $\hat{J}_e \triangleq P_t J_e$. We also define

$$\boldsymbol{v}_t^{\otimes} \triangleq \begin{bmatrix} \boldsymbol{\omega}_t^{\times} & \mathbf{O} \\ \mathbf{v}_t^{\times} & \boldsymbol{\omega}_t^{\times} \end{bmatrix}, \qquad \boldsymbol{v}_t^T \boldsymbol{v}_t^{\otimes} = \mathbf{0} \quad (4)$$

which will be used extensively in the next section. The notation $(\cdot)^{\times}$ denotes the 3×3 skew-symmetric matrix used to implement the vector cross product.

Approximate Motion Equations

Define the payload mass matrix relative to $\mathcal{F}_{N+1}$ by

$$M_t \triangleq \begin{bmatrix} m_t\mathbf{1} & -\mathbf{c}_t^{\times} \\ \mathbf{c}_t^{\times} & \mathbf{J}_t \end{bmatrix} \quad (5)$$

where m_t, $\mathbf{c}_t$, and $\mathbf{J}_t$ are the mass, first, and second moments of inertia respectively. Under the assumptions of invertibility of the rigid Jacobian ($N = 6$) and of the payload being much more massive than the links, it has been shown[16] that the dynamics equation (1) can be well-approximated by

$$M_t\dot{\boldsymbol{v}}_t + \boldsymbol{v}_t^{\otimes} M_t \boldsymbol{v}_t = \hat{J}_\theta^{-T}\boldsymbol{\tau}(t) \quad (6)$$

$$\begin{aligned} \hat{M}_{ee}(\mathbf{q})\ddot{\mathbf{q}}_e + D_{ee}\dot{\mathbf{q}}_e(t) + K_{ee}\mathbf{q}_e(t) \\ = -\hat{J}_e^T\hat{J}_\theta^{-T}\boldsymbol{\tau}(t) + C_e(\mathbf{q}, \dot{\mathbf{q}}_e)\dot{\mathbf{q}}_e \end{aligned} \quad (7)$$

where $\hat{M}_{ee}(\mathbf{q}) \triangleq B_e^T(\mathbf{q})M(\mathbf{q})B_e(\mathbf{q})$ and $B_e^T \triangleq [-J_e^T J_\theta^{-T}\ \mathbf{1}]$. The matrix $\hat{M}_{ee} > \mathbf{O}$ is independent of M_t and the matrix C_e can be chosen so that $2C_e + \dot{\hat{M}}_{ee}$ is skew-symmetric. Assuming that singular configurations are avoided, i.e., J_θ^{-1} exists, it seems reasonable to postulate a lower bound for $\hat{M}_{ee}(\mathbf{q})$. Hence, we also assume that $\hat{M}_{ee} \geq m_{ee}\mathbf{1}$, $0 < m_{ee} < \infty$.

For the duration of the article, Eqs. (6) and (7) will be taken as a valid description of the manipulator dynamics, but our simulation results in section 4 will be based on the exact equations, (1), using a recursive implementation. It has been previously established[16] that the map from $J_\theta^{-T}\boldsymbol{\tau}(t)$ to $\dot{\boldsymbol{\rho}}_\mu$, formed by (6), (7), and the kinematical relations (2) and (3), is passive for $\mu < 1$, i.e.,

$$\int_0^T \dot{\boldsymbol{\rho}}_\mu^T J_\theta^{-T}\boldsymbol{\tau}\, dt \geq -\beta, \quad \beta \geq 0, \quad \forall T > 0$$

where β is constant. (The map is also passive for $\mu = 1$, but the elastic coordinates are not observable from $\dot{\boldsymbol{\rho}}$.) The reader is assumed to be familiar with the notions of passivity and strict passivity as well as the passivity theorem.[20,21] Ortega and Spong[3] provide a summary of these concepts in a robotics context.

Greater insight into the motion equations (6) and (7) and their passivity property can be gleaned by reviewing their origins.[15,16] First consider small undamped motions $\mathbf{q}(t)$ in the neighborhood of a constant setpoint $\bar{\mathbf{q}} = \text{col}\{\bar{\boldsymbol{\theta}}, \mathbf{0}\}$. The undamped linearized forms of (1) and (2) can be obtained by setting $D = \mathbf{O}$, $f_{\text{non}} = \mathbf{0}$, and taking M, J_θ, and J_e to be constant matrices evaluated at $\bar{\mathbf{q}}$. The eigenproblem for the unforced case ($\boldsymbol{\tau} = \mathbf{0}$) yields six zero-frequency rigid modes $\mathbf{q}(t) = B\boldsymbol{\eta}_r(t)$ where $\boldsymbol{\eta}_r(t)$ are the modal coordinates. In addition, the unconstrained vibration modes have frequencies $\omega_\alpha > 0$, $\alpha = 1, 2, 3, \ldots$, and let $\mathbf{q}_\alpha = \text{col}\{\boldsymbol{\theta}_\alpha, \mathbf{q}_{e\alpha}\}$ denote the corresponding eigencolumns. The modal equations of motion follow by letting $\mathbf{q}(t) = B\boldsymbol{\eta}_r(t) + \sum_\alpha \mathbf{q}_\alpha\eta_\alpha(t)$:

$$[B^T MB]\ddot{\eta}_r = \tau = J_\theta^T (J_\theta^{-T}\tau)$$

$$\ddot{\eta}_\alpha + \omega_\alpha^2 \eta_\alpha = (J_\theta \theta_\alpha)^T (J_\theta^{-T}\tau), \quad \alpha = 1, 2, 3, \ldots$$

These equations are valid for *all* payloads in a linear setting.

In the presence of large payloads, it has been previously demonstrated[15] that the flexible motions of the robot (joints unlocked) satisfy clamped boundary conditions at the end-effector: $J_\theta \theta_\alpha + J_e \mathbf{q}_{e\alpha} \doteq 0$, $\alpha = 1, 2, 3, \ldots$, a result which is inescapable on physical grounds alone. Substituting the modal expansion into (2) while noting this property gives

$$\dot{\rho}_\mu = J_\theta \dot{\eta}_r + \sum_\alpha (1 - \mu) J_\theta \theta_\alpha \dot{\eta}_\alpha$$

It is clear that for $\mu = 1$, the elastic modes are unobservable from $\dot{\rho}_\mu = \dot{\rho}$, and the end-effector motion evolves in a purely rigid fashion. For $\mu < 1$, the elastic coordinates become observable (assuming $J_\theta \theta_\alpha \neq 0$), and the map from $J_\theta^{-T}\tau$ to $\dot{\rho}_\mu$ is passive because in the frequency domain the corresponding transfer matrix is positive real.[15]

The nonlinear equation (7) for the elastic coordinates corresponds to (1) with $\dot{\rho} \equiv 0$, i.e., $\dot{\theta} = -J_\theta^{-1} J_e \dot{\mathbf{q}}_e$, as suggested by the modal properties noted above. The end-effector coordinates in (6) are governed by the rigid body dynamics of the payload and are dynamically decoupled from the elastic coordinates. Both approximate equations were originally derived[16] using Lagrangian dynamics in conjunction with a perturbation scheme for the kinetic energy. It is easy to show that the linearized forms of (6) and (7) share the same modal equations as (1) under the large payload assumption. It is the combined rigid/passive nature of the map from $J_\theta^{-T}\tau$ to $\dot{\rho}_\mu|_{\mu=1}$ that makes our adaptive control approach feasible. Preservation of passivity for $\mu < 1$ while creating observability of the elastic coordinates permits their stabilization or, more correctly, prevents their destabilization by the feedback laws. Also required is a feedforward that preserves these properties.

Let $\rho_d(t)$ designate the prescribed end-effector trajectory and define the tracking error $\tilde{\rho} \triangleq \rho - \rho_d$. We assume that $\dot{\rho}_d(t) \to 0$ and $\ddot{\rho}_d(t) \to 0$ as $t \to \infty$ so that $\rho_d(t) \to \bar{\rho}_d$ (a constant). Also define the body-frame quantities $v_d \triangleq P_t(\rho)\dot{\rho}_d$ and

$$\tilde{v}_t \triangleq v_t - v_d = P_t(\rho)\,\dot{\tilde{\rho}} \tag{8}$$

Eq. (6) suggests the feedforward torque

$$\tau_d = \hat{J}_\theta^T(\theta, \mathbf{q}_e)\, W(\dot{v}_d, v_d, v_t)a,$$

$$W(\dot{v}_d, v_d, v_t)a \triangleq [M_t \dot{v}_d + v_d^{\otimes} M_t v_t] \tag{9}$$

It has been parametrized in terms of a regressor matrix W and the true payload mass properties $a \triangleq \text{col}\{m_t, \mathbf{c}_t, \mathcal{J}_t\}$ where $\mathcal{J}_t$ is a column of the 6 independent entries in the payload inertia matrix $\mathbf{J}_t$. The motivation for using v_t instead of v_d in W is the passivity result discussed below.

Define an estimate for the elastic displacements produced by the application of $\tau_d(t)$, $\mathbf{q}_{ed}(t)$, according to the solution of

$$\hat{M}_{ee}(\mathbf{q})\ddot{\mathbf{q}}_{ed} + D_{ee}\dot{\mathbf{q}}_{ed} + K_{ee}\mathbf{q}_{ed} = -\hat{J}_e^T \hat{J}_\theta^{-T}\tau_d + C_e(\mathbf{q}, \dot{\mathbf{q}}_e)\dot{\mathbf{q}}_{ed} \tag{10}$$

The reference trajectory for ρ_μ, $\rho_{\mu d}$, is defined by its time derivative as suggested by (2),

$$\dot{\rho}_{\mu d} = \dot{\rho}_d - (1 - \mu) J_e(\theta, \mathbf{q}_e)\dot{\mathbf{q}}_{ed} \tag{11}$$

and the corresponding tracking errors $\tilde{\rho}_\mu \triangleq \rho_\mu - \rho_{\mu d}$ satisfy

$$\dot{\tilde{\rho}}_\mu = \dot{\tilde{\rho}} - (1 - \mu) J_e \dot{\tilde{\mathbf{q}}}_e, \; \tilde{\mathbf{q}}_e \triangleq \mathbf{q}_e - \mathbf{q}_{ed} \tag{12}$$

It can also be shown[16] that the map from $J_\theta^{-T}(\tau - \tau_d)$ to $\dot{\tilde{\rho}}_\mu(t)$ is passive. Therefore, stabilization and tracking can be accomplished by taking the feedback portion of τ, $\tilde{\tau} \triangleq \tau - \tau_d$, to be the product of J_θ^T and a strictly passive function of $\dot{\tilde{\rho}}_\mu(t)$. In the next section, we modify (9) and develop its adaptive counterpart by introducing an appropriate filtered error.

3. ADAPTIVE CONTROLLER

Fixed Parameter Control Law

The above results possess the basic features for extending rigid adaptive controllers[3–5] to the flexible case. These are the passivity property and the linear dependence of the feedforward law (9) on the unknown parameters. Like the rigid case,[1] it must be modified to ensure stable tracking of the position errors. To this end, define the filtered body frame rates by

$$v_r(t) \triangleq v_d(t) - P_t(\rho)\Lambda\tilde{\rho}_\mu(t) = P_t[\dot{\rho}_d - \Lambda\tilde{\rho}_\mu] \tag{13}$$

where $\Lambda = \Lambda^T > \mathbf{O}$. Furthermore, we define

$$s_\mu \triangleq \dot{\tilde{\rho}}_\mu + \Lambda\tilde{\rho}_\mu \tag{14}$$

and make the standard observation[3] that $s_\mu \in L_2$ implies that $\tilde{\rho}_\mu(t) \in L_2 \cap L_\infty$, $\dot{\tilde{\rho}}_\mu(t) \in L_2$, and $\tilde{\rho}_\mu(t) \to 0$ as $t \to \infty$. Furthermore, if $s_\mu(t) \to 0$ as $t \to \infty$, then $\dot{\tilde{\rho}}_\mu(t) \to 0$.

Now replace $\boldsymbol{v}_d(t)$ with $\boldsymbol{v}_r(t)$ in the fixed parameter feedforward (9) which gives

$$\boldsymbol{\tau}_d = \hat{\boldsymbol{J}}_\theta^T \boldsymbol{W}(\dot{\boldsymbol{v}}_r, \boldsymbol{v}_r, \boldsymbol{v}_t)\boldsymbol{a} \tag{15}$$

and it is assumed that $\mathbf{q}_{ed}$ remains defined by (10) but with $\boldsymbol{\tau}_d$ as given above. Subtracting (15) from (6) and (10) from (7) gives the following description of the error dynamics:

$$\boldsymbol{M}_t\dot{\tilde{\boldsymbol{v}}}_r + \tilde{\boldsymbol{v}}_r^{\otimes}\boldsymbol{M}_t\boldsymbol{v}_t = \hat{\boldsymbol{J}}_\theta^{-T}\tilde{\boldsymbol{\tau}},\ \tilde{\boldsymbol{\tau}} \triangleq \boldsymbol{\tau} - \boldsymbol{\tau}_d \tag{16}$$

$$\hat{\boldsymbol{M}}_{ee}(\mathbf{q})\ddot{\tilde{\mathbf{q}}}_e + \boldsymbol{D}_{ee}\dot{\tilde{\mathbf{q}}}_e + \boldsymbol{K}_{ee}\tilde{\mathbf{q}}_e = -\hat{\boldsymbol{J}}_e^T\hat{\boldsymbol{J}}_\theta^{-T}\tilde{\boldsymbol{\tau}} + \boldsymbol{C}_e(\mathbf{q}, \dot{\mathbf{q}}_e)\dot{\tilde{\mathbf{q}}}_e,\ \tilde{\mathbf{q}}_e = \mathbf{q}_e - \mathbf{q}_{ed} \tag{17}$$

where $\tilde{\boldsymbol{v}}_r \triangleq \boldsymbol{v}_t - \boldsymbol{v}_r = \tilde{\boldsymbol{v}}_t + \boldsymbol{P}_t\boldsymbol{\Lambda}\tilde{\boldsymbol{\rho}}_\mu = \boldsymbol{P}_t[\dot{\tilde{\boldsymbol{\rho}}} + \boldsymbol{\Lambda}\tilde{\boldsymbol{\rho}}_\mu]$. We now show that the passivity property is maintained by the new feedforward but with respect to the filtered output $\boldsymbol{s}_\mu$.

Lemma 1. *The mapping $\boldsymbol{s}_\mu = \boldsymbol{G}(\boldsymbol{J}_\theta^{-T}\tilde{\boldsymbol{\tau}})$, where $\boldsymbol{G}$ is determined by (11)–(17), is passive for $\mu < 1$.*

Proof. Define the nonnegative function

$$\mathcal{V}_\mu = \tfrac{1}{2}\tilde{\boldsymbol{v}}_r^T\boldsymbol{M}_t\tilde{\boldsymbol{v}}_r + \tfrac{1}{2}(1-\mu)[\dot{\tilde{\mathbf{q}}}_e^T\hat{\boldsymbol{M}}_{ee}\dot{\tilde{\mathbf{q}}}_e + \tilde{\mathbf{q}}_e^T\boldsymbol{K}_{ee}\tilde{\mathbf{q}}_e],\quad \mu < 1 \tag{18}$$

Differentiating the above with respect to time and using (16), (17), and the skew-symmetry of $2\boldsymbol{C}_e + \dot{\hat{\boldsymbol{M}}}_{ee}$ gives

$$\begin{aligned}\dot{\mathcal{V}}_\mu &= \tilde{\boldsymbol{v}}_r^T\boldsymbol{M}_t\dot{\tilde{\boldsymbol{v}}}_r + (1-\mu)\dot{\tilde{\mathbf{q}}}_e^T[\hat{\boldsymbol{M}}_{ee}(\mathbf{q})\ddot{\tilde{\mathbf{q}}}_e + \boldsymbol{K}_{ee}\tilde{\mathbf{q}}_e + \tfrac{1}{2}\dot{\hat{\boldsymbol{M}}}_{ee}\dot{\tilde{\mathbf{q}}}_e]\\ &= \tilde{\boldsymbol{v}}_r^T[-\tilde{\boldsymbol{v}}_r^{\otimes}\boldsymbol{M}_t\boldsymbol{v}_t + \hat{\boldsymbol{J}}_\theta^{-T}\tilde{\boldsymbol{\tau}}] - (1-\mu)\dot{\tilde{\mathbf{q}}}_e^T[\hat{\boldsymbol{J}}_e^T\hat{\boldsymbol{J}}_\theta^{-T}\tilde{\boldsymbol{\tau}} + \boldsymbol{D}_{ee}\dot{\tilde{\mathbf{q}}}_e]\end{aligned}$$

Then, using the property (4) and the definition in (12) yields

$$\begin{aligned}\dot{\mathcal{V}}_\mu &= [\tilde{\boldsymbol{v}}_r - (1-\mu)\hat{\boldsymbol{J}}_e\dot{\tilde{\mathbf{q}}}_e]^T\hat{\boldsymbol{J}}_\theta^{-T}\tilde{\boldsymbol{\tau}} - (1-\mu)\dot{\tilde{\mathbf{q}}}_e^T\boldsymbol{D}_{ee}\dot{\tilde{\mathbf{q}}}_e\\ &= \boldsymbol{s}_\mu^T(\boldsymbol{J}_\theta^{-T}\tilde{\boldsymbol{\tau}}) - (1-\mu)\dot{\tilde{\mathbf{q}}}_e^T\boldsymbol{D}_{ee}\dot{\tilde{\mathbf{q}}}_e\end{aligned} \tag{19}$$

Integrating the above relationship gives $\int_0^T \boldsymbol{s}_\mu^T(\boldsymbol{J}_\theta^{-T}\tilde{\boldsymbol{\tau}})\,dt \geq \mathcal{V}_\mu(T) - \mathcal{V}_\mu(0)$ which establishes the passivity property upon noting that $\mathcal{V}_\mu(T) \geq 0$ for $\mu < 1$. ∎

Adaptive Version

It is now reasonably straightforward to apply the techniques of the rigid case to the present situation.

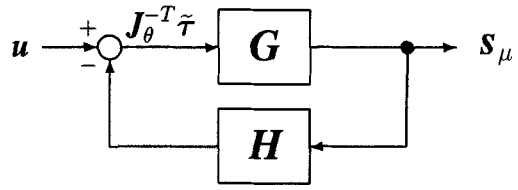

Figure 1. Feedback system.

With reference to the feedback system in Figure 1, one form of the passivity theorem[20] (see Theorem VI.5.1 in ref. 20) states that if $\boldsymbol{G}$: $L_{2e} \to L_{2e}$ is passive and $\boldsymbol{H}$: $L_{2e} \to L_{2e}$ is strictly passive then the system is L_2-stable, i.e., if $\mathbf{u} \in L_2$ (an energy-bounded disturbance torque) then $\boldsymbol{s}_\mu \in L_2$. Based on the passivity theorem, we should select the feedback portion of the controller such that

$$\tilde{\boldsymbol{\tau}} = -\boldsymbol{J}_\theta^T(\boldsymbol{\theta}, \mathbf{q}_e)\boldsymbol{H}(\boldsymbol{s}_\mu),\quad \int_0^T \boldsymbol{s}_\mu^T\boldsymbol{H}(\boldsymbol{s}_\mu)\,dt \geq \varepsilon\int_0^T \boldsymbol{s}_\mu^T\boldsymbol{s}_\mu\,dt - \beta,\ \forall T > 0 \tag{20}$$

for some constant $\beta \geq 0$ and $\varepsilon > 0$, i.e., $\boldsymbol{H}$ is strictly passive.

Since $\boldsymbol{a}$ is unknown, let us take the applied torque to be

$$\boldsymbol{\tau}(t) = \hat{\boldsymbol{J}}_\theta^T\boldsymbol{W}(\dot{\boldsymbol{v}}_r, \boldsymbol{v}_r, \boldsymbol{v}_t)\hat{\boldsymbol{a}}(t) + \bar{\boldsymbol{\tau}}(t) \tag{21}$$

where $\hat{\boldsymbol{a}}$ are the estimated payload parameters and $\bar{\boldsymbol{\tau}}$ is the feedback part of the controller to be identified. Subtracting (15) from (21) yields

$$\tilde{\boldsymbol{\tau}} = \boldsymbol{\tau} - \boldsymbol{\tau}_d = \hat{\boldsymbol{J}}_\theta^T\boldsymbol{W}\tilde{\boldsymbol{a}} + \bar{\boldsymbol{\tau}},\ \tilde{\boldsymbol{a}}(t) \triangleq \hat{\boldsymbol{a}}(t) - \boldsymbol{a} \tag{22}$$

and hence

$$\int_0^T (\boldsymbol{J}_\theta^{-T}\tilde{\boldsymbol{\tau}})^T\boldsymbol{s}_\mu\,dt = \int_0^T \tilde{\boldsymbol{a}}^T\boldsymbol{W}^T\boldsymbol{P}_t\boldsymbol{s}_\mu\,dt + \int_0^T (\boldsymbol{J}_\theta^{-T}\bar{\boldsymbol{\tau}})^T\boldsymbol{s}_\mu\,dt \tag{23}$$

If $\tilde{\boldsymbol{a}}$ is chosen to be a passive function of $-\boldsymbol{W}^T\boldsymbol{P}_t\boldsymbol{s}_\mu(t)$ and the map from $-\boldsymbol{s}_\mu$ to $\boldsymbol{J}_\theta^{-T}\bar{\boldsymbol{\tau}}$ is strictly passive, (20) will be satisfied.

Based on these observations, we take

$$\boldsymbol{\tau}(t) = \hat{\boldsymbol{J}}_\theta^T\boldsymbol{W}(\dot{\boldsymbol{v}}_r, \boldsymbol{v}_r, \boldsymbol{v}_t)\hat{\boldsymbol{a}}(t) - \boldsymbol{J}_\theta^T\mathbf{K}_d\boldsymbol{s}_\mu,\quad \mathbf{K}_d = \mathbf{K}_d^T > \mathbf{O} \tag{24}$$

$$\dot{\hat{\boldsymbol{a}}}(t) = \dot{\tilde{\boldsymbol{a}}}(t) = -\boldsymbol{\Gamma}\boldsymbol{W}^T\boldsymbol{P}_t\boldsymbol{s}_\mu,\ \boldsymbol{\Gamma} = \boldsymbol{\Gamma}^T > \mathbf{O} \tag{25}$$

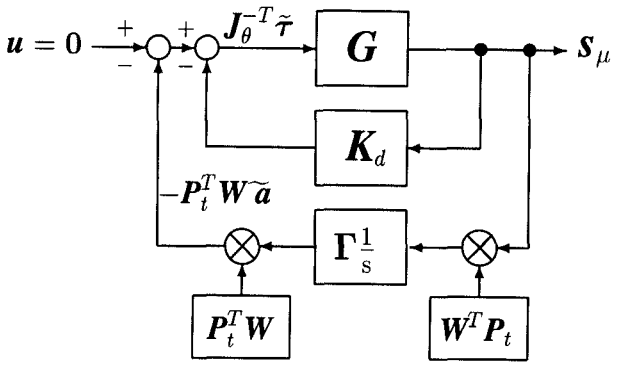

Figure 2. Adaptive controller.

i.e., $J_\theta^{-T}\tilde{\tau} = -\mathbf{K}_d s_\mu$. We have used the simplest passive adaptation law which avoids the explicit appearance of the true parameters (an integrator), and the simplest strictly passive feedback, namely a constant positive-definite gain matrix. Clearly, more general choices are possible on the basis of the above arguments. The overall system is shown in Figure 2 and can be interpreted as the feedback interconnection of a passive system (G) and a strictly passive system. Hence, $s_\mu \in L_2$ and, therefore, so are $\tilde{\rho}_\mu\ \dot{\tilde{\rho}}_\mu \in L_2$. To establish asymptotic tracking of the true tip rate and position errors, we present a Lyapunov argument.

Theorem 1. *The adaptive system described by (16), (17), (24) and (25) yields global asymptotic stability for the tracking errors $\tilde{\rho}$ and $\dot{\tilde{\rho}}$.*

Proof. We adopt as a Lyapunov function

$$V(t) = \mathcal{S}_\mu + \tfrac{1}{2}\tilde{a}^T\Gamma^{-1}\tilde{a} \geq 0 \tag{26}$$

where $\mathcal{S}_\mu$ is defined by (18). Using (19), (22), (24), and (25), we have

$$\begin{aligned}\dot{V} &= \dot{\mathcal{S}}_\mu + \tilde{a}^T\Gamma^{-1}\dot{\tilde{a}} \\ &= s_\mu^T J_\theta^{-T}\tilde{\tau} - (1-\mu)\dot{\tilde{\mathbf{q}}}_e^T D_{ee}\dot{\tilde{\mathbf{q}}}_e - \tilde{a}^T W^T P_t s_\mu \\ &= s_\mu^T[J_\theta^{-T}\tilde{\tau} - P_t^T W\tilde{a}] - (1-\mu)\dot{\tilde{\mathbf{q}}}_e^T D_{ee}\dot{\tilde{\mathbf{q}}}_e \\ &= -s_\mu^T\mathbf{K}_d s_\mu - (1-\mu)\dot{\tilde{\mathbf{q}}}_e^T D_{ee}\dot{\tilde{\mathbf{q}}}_e \leq 0\end{aligned} \tag{27}$$

Hence, we conclude that $s_\mu \in L_2 \cap L_\infty$, $\dot{\tilde{\mathbf{q}}}_e \in L_2 \cap L_\infty$, and therefore $\dot{\tilde{\rho}}_\mu \in L_2$, $\tilde{\rho}_\mu \in L_2 \cap L_\infty$, and $\tilde{\rho}_\mu(t) \to \mathbf{0}$ as $t \to \infty$. Since $V(t)$ is bounded, $\tilde{a}$, $\tilde{\mathbf{q}}_e$, $\dot{\tilde{\mathbf{q}}}_e$, and $\tilde{v}_r$ are also bounded and so is $\dot{\tilde{\rho}}$ (hence $\tilde{\rho}$ and $\dot{\tilde{\rho}}_\mu$). This makes v_r, $\dot{v}_r$, v_t, W, and hence $\tilde{\tau}$ bounded. From the error dynamics (16) and (17), $\dot{\tilde{v}}_r = \dot{P}_t(\dot{\tilde{\rho}} + \Lambda\tilde{\rho}_\mu) + P_t(\ddot{\tilde{\rho}} + \Lambda\dot{\tilde{\rho}}_\mu)$ and $\ddot{\tilde{\mathbf{q}}}_e$ are bounded. This makes $\dot{s}_\mu = \ddot{\tilde{\rho}}_\mu + \Lambda\dot{\tilde{\rho}}_\mu$ bounded and, hence, s_μ and $\dot{\tilde{\mathbf{q}}}_e$ are uniformly continuous. Thus, as $t \to \infty$, $\dot{\tilde{\mathbf{q}}}_e(t) \to \mathbf{0}$, $\tilde{\mathbf{q}}_e$ becomes constant, $s_\mu(t) \to \mathbf{0}$, and therefore $\dot{\tilde{\rho}}_\mu(t) \to \mathbf{0}$. Because $\dot{\tilde{\rho}}_\mu(t) \to \mathbf{0}$ and $\dot{\tilde{\mathbf{q}}}_e(t) \to \mathbf{0}$, the true tip rate tracking errors $\dot{\tilde{\rho}}(t) \to \mathbf{0}$ as $t \to \infty$.

It remains to show that the tip position errors are asymptotically zero. Since $\dot{\rho}_d$, $\ddot{\rho}_d$, $\tilde{\rho}_\mu$, and $\dot{\tilde{\rho}}_\mu$ all vanish as $t \to \infty$, then from (13), $v_r(t) \to \mathbf{0}$, $\dot{v}_r(t) \to \mathbf{0}$, and hence $W(\dot{v}_r, v_r, v_t)$ in (22) must vanish as $t \to \infty$. Therefore, using (22) and (24) *et seq.*, $\tilde{\tau}(t) \to \mathbf{0}$ as $t \to \infty$, and we conclude from (17) that $\tilde{\mathbf{q}}_e \to \mathbf{0}$. Since $\tilde{\rho}_\mu(t) \to \mathbf{0}$ and $\tilde{\mathbf{q}}_e(t) \to \mathbf{0}$, the tracking errors $\tilde{\rho}(t) \to \mathbf{0}$ as $t \to \infty$. A simpler alternative proof uses the fact that $\mathcal{V}$ is positive-definite in the state $\text{col}\{\dot{\tilde{\rho}}, \dot{\tilde{\mathbf{q}}}_e, \tilde{\rho}, \tilde{\mathbf{q}}_e, \tilde{a}\}$ and makes use of LaSalle's extension for nonautonomous systems which are asymptotically autonomous.[22] Note that the invariant set consistent with $\dot{\mathbf{q}} \equiv \mathbf{0}$ is given by $s_\mu = \dot{\tilde{\mathbf{q}}}_e \equiv \mathbf{0}$. This coupled with (16), (17), (22), (24), and (25) implies that $\dot{\tilde{\rho}} = \tilde{\rho} \equiv \mathbf{0}$. ∎

Based on the above, $W\tilde{a} \to \mathbf{0}$ but, as usual, $\tilde{a} \to \mathbf{0}$ cannot be concluded unless W satisfies a persistency of excitation condition.

In general, construction of $\dot{\rho}_\mu$ and ρ_μ requires direct measurement of the elastic coordinates $\mathbf{q}_e$ which are required in the evaluation of the Jacobian matrix $J_\theta(\theta, \mathbf{q}_e)$ and the formation of the μ-tip positions and rates. If the rigid Jacobian is approximated by $J_\theta(\theta, \mathbf{0})$ ($\hat{J}_\theta(\theta, \mathbf{0})$ in the feedforward part of the controller) and $\dot{\rho}_{\mu d} \doteq \dot{\rho}_d$ then

$$\begin{aligned}\dot{\tilde{\rho}}_\mu(t) &= \dot{\rho}_\mu - \dot{\rho}_{\mu d} \\ &\doteq [\mu\,\dot{\rho}(t) + (1-\mu)J_\theta(\theta, \mathbf{0})\,\dot{\theta}(t)] - \dot{\rho}_d(t)\end{aligned} \tag{28}$$

By setting $\dot{\rho}_{\mu d} \doteq \dot{\rho}_d$ (hence $\rho_{\mu d} \doteq \rho_d$), we are rid of the need to construct $\mathbf{q}_{ed}$ and $\dot{\mathbf{q}}_{ed}$ using (10). This is justified on the grounds that our numerical results indicate that an appropriate value for μ is nearly 1. The μ-tip position error can be determined from the integral of (28):

$$\tilde{\rho}_\mu(t) = [\mu\rho(t) + (1-\mu)F(\theta)] - \rho_d(t) \tag{29}$$

where, recall, $F(\theta)$ represents the rigid forward kinematics map.

Hence $\tilde{\rho}_\mu$ and its time derivative can be constructed from the joint measurements $\{\theta(t), \dot{\theta}(t)\}$, tip measurements $\{\rho(t), \dot{\rho}(t)\}$, and the prescribed Cartesian trajectory. This is significant because the elastic coordinates are numerous and can be difficult to

sense. Furthermore, their interpretation depends on the specifics of the spatial discretization that is adopted. A further simplification is possible if we replace $P_t(\rho)$ with $P_t(\rho_d)$ in calculating v_r and $\dot{v}_r$ using (13) and $\hat{a}$ in (25). These changes will be incorporated into the following summary of the adaptive controller implementation.

Summary of the Adaptive Controller

At time t, the following calculations are made:

1. Given the measurements $\{\theta(t), \dot{\theta}(t), \rho(t), \dot{\rho}(t)\}$ and the prescribed values $\dot{\rho}_d(t)$, $\rho_d(t)$, form the tracking errors $\dot{\tilde{\rho}}_\mu(t)$ using (28) and $\tilde{\rho}_\mu(t)$ using (29).
2. Form

$$s_\mu(t) = \dot{\tilde{\rho}}_\mu(t) + \Lambda\tilde{\rho}_\mu(t)$$

$$v_t(t) = P_t(\rho)\dot{\rho}(t)$$

$$v_r(t) = P_t(\rho_d)[\dot{\rho}_d(t) - \Lambda\tilde{\rho}_\mu(t)]$$

$$\dot{v}_r(t) = \dot{P}_t(\rho_d)P_t^{-1}(\rho_d)v_r(t) + P_t(\rho_d)[\ddot{\rho}_d(t) - \Lambda\dot{\tilde{\rho}}_\mu(t)]$$

3. Given the parameter update $\hat{a}(t)$, calculate $\hat{M}_t$ (the estimated payload mass matrix). Using (24) and (9), the applied torque becomes

$$\tau(t) = \hat{J}_\theta^T(\theta, 0)[\hat{M}_t\dot{v}_r(t) + v_r^{\otimes}(t)\hat{M}_t v_t(t)] - \hat{J}_\theta^T(\theta, 0)K_d s_\mu(t) \quad (30)$$

4. Calculate $\dot{\hat{a}}(t) = -W^T(\dot{v}_r, v_r, v_t)P_t(\rho_d)s_\mu$ and estimate $\hat{a}(t + \Delta t)$ using some quadrature scheme.

These calculations are no more onerous than those corresponding to the task space adaptive controllers that have been suggested for rigid arms.[1,23] The regressor matrix is particularly simple because it depends only on the body-frame dynamics of the payload, not those governing the entire manipulator. The only Jacobian matrix required is the usual rigid one, and its inverse need not be calculated. For $\mu = 1$, the feedforward is formally the same as that advocated by Fossen[24] in the context of spacecraft attitude control. He pointed out the advantages of using the body frame over the inertial frame for the regressor parametrization. It is also worth pointing out the similarity of the feedback portion to the task space feedback strategy of Miyazaki and Arimoto[25] for rigid arms. For $\mu = 1$, the feedback part of (30) is identical to their "sensory PD feedback" which they showed has certain advantages over inverse Jacobian methods. We have used the inertial frame for the feedback part of the controller since $\dot{\rho}$ is integrable whereas v_t is not. The primary reason for taking $\mu < 1$ is the introduction of the elastic modes (which are unobservable when $\mu = 1$)[15] into the controller input.

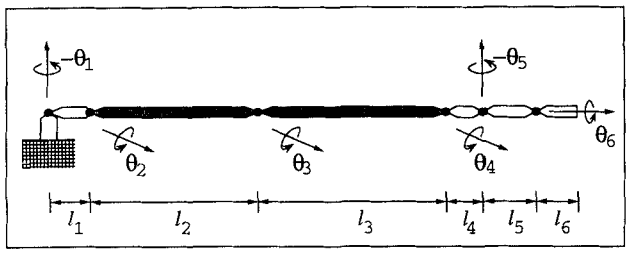

Figure 3. Flexible manipulator model.

4. NUMERICAL EXAMPLE

We now implement the proposed controller in a simulation based on the full motion equations. The system model is based on the Space Shuttle Remote Manipulator (SRMS) Arm and possesses six joints. The system is depicted in Figure 3 and has been previously studied in other contexts[16,26] (see these references for the mass and geometric properties). All links have uniform tubular cross-sections and are taken as rigid with the exception of links 2 and 3. These long booms are modeled as flexible, and the exact cantilevered eigenfunctions are used for discretization. We use six modes per boom: two bending modes in each transverse plane, one stretch mode, and one torsional mode. A complete description of their elastic properties as well as the dynamics equations underlying the simulation appears elsewhere[26] (we use the **EEE** model of this reference). The cantilevered natural frequencies are given in Table 1. All inertial nonlinearities are included, including the elastic configuration dependence in the global mass matrix.

Table 1. Cantilevered natural frequencies (rad/s).

	First bending mode	Second bending mode	First stretch mode	First torsional mode
Link 2	37.18	233.0	2791.	1401.
Link 3	34.53	216.4	2224.	1116.

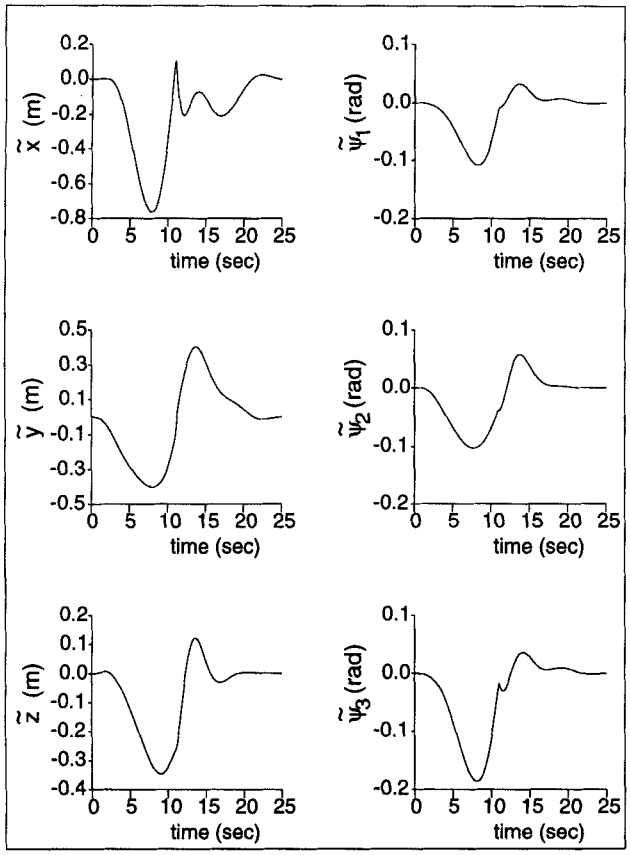

Figure 4. Tip position tracking errors (PD Law).

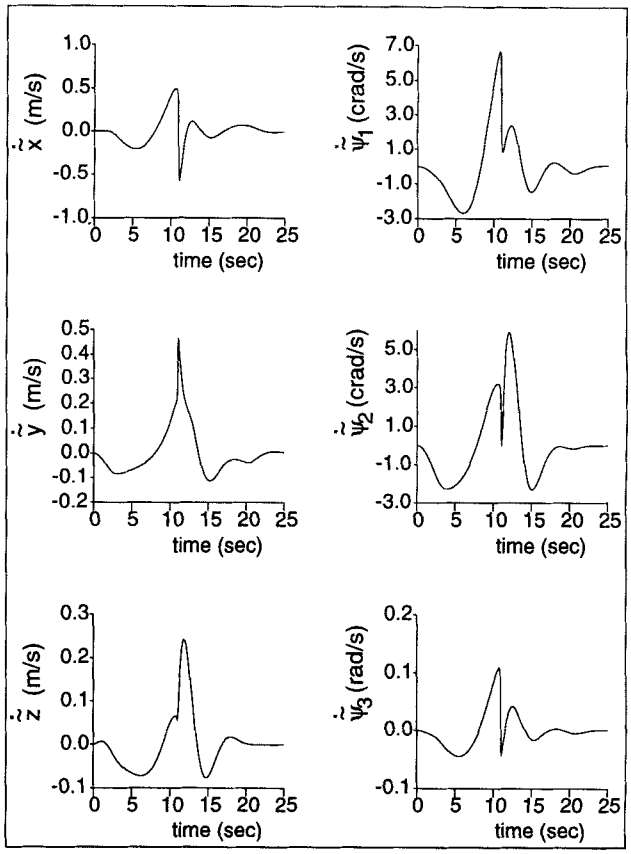

Figure 5. Tip rate tracking errors (PD Law).

Structural damping is neglected in the simulation ($D_{ee} = \mathbf{O}$). The total mass of the links is 411 kg, and their fully extended length is 16.2 m. A payload is cantilevered at the end-effector with the following mass properties: $m_t = 15{,}000$ kg, $\mathbf{c}_t = [75{,}000\ 0\ 0]^T$ kg · m, and $\mathbf{J}_t = \text{diag}\{30, 515, 515\} \times 10^3$ kg · m^2 (the x-axis is aligned with the axial direction of link 6). The initial configuration corresponds to $\boldsymbol{\theta}(0) = \mathbf{0}$ (the datum shown in Figure 3), and the desired terminal configuration is $\theta_n(T) = 0.4$ rad, $n = 1 \ldots 6$, where $T = 20$ sec. The prescribed trajectory $\{\boldsymbol{\rho}_d(t), \dot{\boldsymbol{\rho}}_d(t)\}$ is fashioned from the rigid forward kinematic solution corresponding to the joint trajectories $\theta_n(t) = \theta_n(T)[t/T - (2\pi)^{-1} \sin(2\pi t/T)]$. A 3-2-1 Euler sequence $\{\psi_1, \psi_2, \psi_3\}$ is used to characterize the end-effector orientation.

The feedback matrices are selected as follows: $\mathbf{K}_d = \Omega_c \mathbf{P}_t^T(\bar{\boldsymbol{\rho}}_d) \mathbf{M}_t \mathbf{P}_t(\bar{\boldsymbol{\rho}}_d)$ and $\boldsymbol{\Lambda} = \Omega_c \mathbf{1}$ where $\Omega_c = 1$ rad/s. The matrix $\boldsymbol{\Gamma}$ is taken to be diagonal with entries

$$\boldsymbol{\Gamma}_{mm} = 10\Omega_c \Big/ \left[\int_0^T \mathbf{W}^T(\dot{\boldsymbol{v}}_d, \boldsymbol{v}_d, \boldsymbol{v}_d) \overline{\mathbf{K}}_d^{-1} \mathbf{W}(\dot{\boldsymbol{v}}_d, \boldsymbol{v}_d, \boldsymbol{v}_d)\, dt \right]_{mm}, \quad m = 1 \ldots 10$$

where $\overline{\mathbf{K}}_d$ is the diagonal part of $\mathbf{K}_d$. The value of μ is taken to be 0.99.

The tip position tracking errors $\tilde{\boldsymbol{\rho}}$, $\boldsymbol{\rho}(t) = [x\ y\ z\ \psi_1\ \psi_2\ \psi_3]^T$, and tip rate tracking errors $\dot{\tilde{\boldsymbol{\rho}}}$ are plotted in Figures 4–7. Three cases are illustrated: the PD feedback alone ($\hat{\boldsymbol{a}} \equiv \mathbf{0}$), the fixed parameter form of (24) ($\hat{\boldsymbol{a}} \equiv \boldsymbol{a}$), and the adaptive case with $\hat{\boldsymbol{a}}(0) = \mathbf{0}$. As an aid in interpreting the errors, the maximum absolute value of each prescribed Cartesian variable is given in Table 2. Although the PD law alone performs reasonably well, the two cases with feedforward perform much better. The fixed parameter form yields RMS position errors that are at least ten times smaller. Interestingly, the adaptive law outperforms

Table 2. Maximum absolute values of prescribed trajectory.

$\lvert x_d \rvert_{\max}$	16.2 m	$\lvert \dot{x}_d \rvert_{\max}$	0.637 m/s
$\lvert y_d \rvert_{\max}$	9.18 m	$\lvert \dot{y}_d \rvert_{\max}$	0.959 m/s
$\lvert z_d \rvert_{\max}$	5.30 m	$\lvert \dot{z}_d \rvert_{\max}$	0.600 m/s
$\lvert \psi_{1d} \rvert_{\max}$	0.83 rad	$\lvert \dot{\psi}_{1d} \rvert_{\max}$	9.39 crad/s
$\lvert \psi_{2d} \rvert_{\max}$	0.51 rad	$\lvert \dot{\psi}_{2d} \rvert_{\max}$	6.53 crad/s
$\lvert \psi_{3d} \rvert_{\max}$	1.39 rad	$\lvert \dot{\psi}_{3d} \rvert_{\max}$	0.14 rad/s

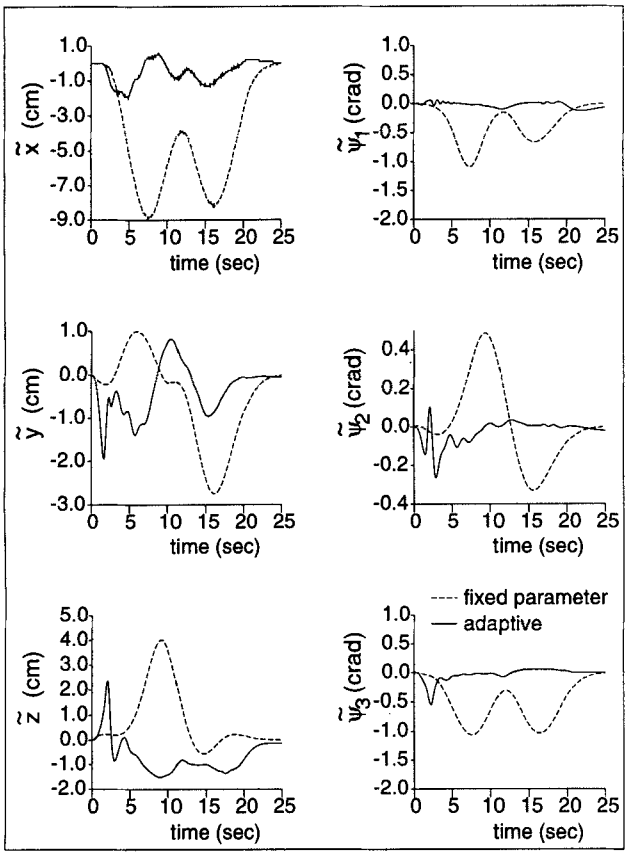

Figure 6. Tip position tracking errors.

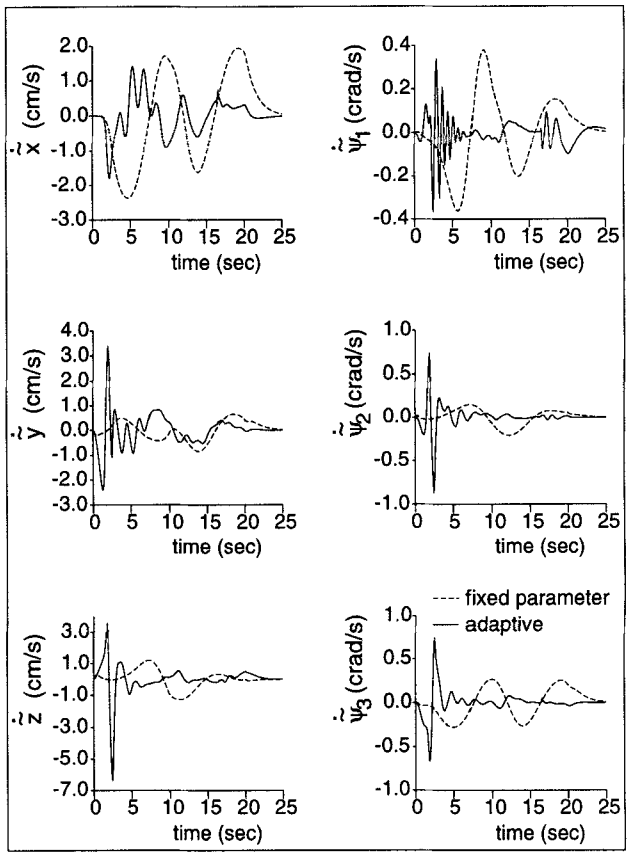

Figure 7. Tip rate tracking errors.

the fixed parameter form on which it is based (the RMS position errors are about four times smaller). This is attributed to the approximate nature of the underlying motion equations, (6) and (7), which are used for its design. The adaptation appears to surmount the errors induced by inaccuracies in the feedforward model and yields excellent tracking.

The time evolution of some of the parameter estimates is given in Figure 8. As might be expected, they do not converge to the true values given the simple nature of the prescribed trajectory. Each of the simulations was carried out for various values of the true payload properties. Stable behavior with good tracking was observed for payloads as small as m_t = 1500 kg (linear scaling of $\mathbf{c}_t$ and $\mathbf{J}_t$) which is only four times larger than the manipulator. The tracking errors in this case are very similar to those in Figures 6 and 7 for the larger payload. When the payload mass was reduced to 375 kg (less than the total manipulator mass), the adaptive controller went unstable owing to divergence of the parameter estimates. This is easily explained by the "unmodeled rigid dynamics" (everything but the payload)

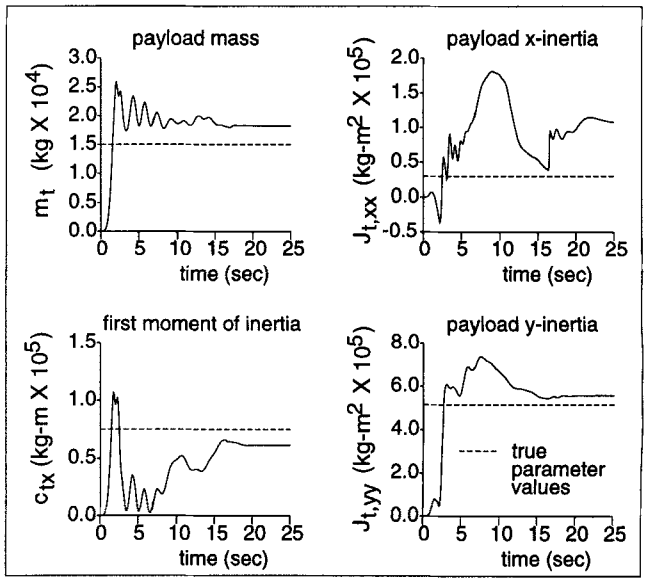

Figure 8. Payload parameter estimates.

which is quite significant when the payload mass is comparable to that of the robot.

5. CONCLUSIONS

Based on an approximate set of dynamics equations, an adaptive controller has been developed for a flexible manipulator carrying a large uncertain payload. Given these motion equations, globally stable tracking of the end-effector was established. By exploiting the passive nature of the μ-tip rates, many of the techniques introduced in the rigid setting were exploited for flexible arms. The ensuing controllers have a simple structure and do not require sensing of the elastic coordinates or their rates.

Our simulation results illustrated the stability properties with respect to the full nonlinear equations of motion. Excellent tracking of all six Cartesian variables was observed. This lends further credence to the approximate motion equations underlying the controller development. Although the large payload assumption may seem restrictive, there are many applications in the space environment where it is satisfied. The numerical results show that it can be significantly relaxed and still produce good controller performance. Although structural damping was required for the stability proof, its absence in the simulation did not seem particularly troublesome.

Because the controller design is based on the passivity theorem, there exist many alternatives to the feedback laws used here. In particular, the integral adaptation law can be replaced with an integrator plus an arbitrary positive real transfer matrix. Additionally, the positive-definite feedback gain $\mathbf{K}_d$ can be replaced with a dynamic controller which is strictly positive real. These options open the door to further potential performance enhancements.

REFERENCES

1. J.-J. E. Slotine and W. Li, "On the adaptive control of robot manipulators," *Int. J. Robotics Research,* **6**(3), 49–59, 1987.
2. N. Sadegh and R. Horowitz, "Stability analysis of a class of adaptive controllers for robotic manipulators," *Int. J. Robotics Res.,* **9**(3), 74–92, 1990.
3. R. Ortega and M. W. Spong, "Adaptive motion control of rigid robots: a tutorial," *Automatica,* **25,** 877–888, 1989.
4. I. Landau and R. Horowitz, "Applications of the passive systems approach to the stability analysis of adaptive controllers for robot manipulators," *Int. J. Adapt. Control Signal Process.,* **3,** 23–38, 1989.
5. R. Kelly, R. Carelli, and R. Ortega, "Adaptive motion control design of robot manipulators: an input-output approach," *Int. J. Control,* **50**(6), 2563–2581, 1989.
6. A. De Luca, P. Lucibello, and G. Ulivi, "Inversion techniques for trajectory control of flexible robot arms," *J. Robotic Syst.* **6**(4), 325–344, 1989.
7. L. Lanari and J. Wen, "A family of asymptotically stable control laws for flexible robots based on a passivity approach," CIRSSE Report 85, Rennselaer Polytechnic Institute, February 1991.
8. A. De Luca and B. Siciliano, "Inversion-based nonlinear control of robot arms with flexible links," *AIAA J. Guid. Control Dyn.,* **16**(6), 1169–1176, 1993.
9. M. W. Spong, "Adaptive control of flexible joint manipulators," *Syst. Control Lett.,* **13,** 15–21, 1989.
10. K. Khorasani, "Adaptive control of flexible-joint robots," *IEEE Trans. Rob. Autom.,* **8**(2), 250–267, 1992.
11. R. Lozano and B. Brogliato, "Adaptive control of robot manipulators with flexible joints," *IEEE Trans. Autom. Control,* **37**(2), 174–181, 1992.
12. B.-S. Yuan, W. J. Book, and B. Siciliano, "Direct adaptive control of a one-link flexible arm with tracking," *J. Robotic Syst.,* **6**(6), 663–680, 1989.
13. V. Feliu, K. S. Rattan, and H. B. Brown, Jr., "Adaptive control of a single-link flexible manipulator in the presence of joint friction and load changes," *Proc. 1989 IEEE Int. Conf. Robotics Automat.,* Scottsdale, AZ, 1036-1041, 1989.
14. C. M. Pham, W. Khalil, and C. Chevallereau, "A nonlinear model-based control of flexible robots," *Robotica,* **11,** 73–82, 1993.
15. C. J. Damaren, "Passivity analysis for flexible multilink space manipulators," *AIAA J. Guid. Control, Dyn.,* **18**(2), 272–279, 1995.
16. C. J. Damaren, "Approximate inverse dynamics and passive feedback for flexible manipulators with large payloads," *IEEE Trans. Rob. Autom.,* (To appear) **12**(1), 1996.
17. D. Wang and M. Vidyasagar, "Passive Control of a Single Flexible Link," *Proc. 1990 IEEE Int. Conf. Rob. Automat.,* Cincinnati, OH, 1432-1437, May 1990.
18. G. B. Sincarsin and P. C. Hughes, "Dynamics of elastic multibody chains: Part A—body motion equations," *Dyn. Stab. Syst.,* **4,** 209–226, 1990.
19. P. C. Hughes and G. B. Sincarsin, "Dynamics of elastic multibody chains: Part B—global dynamics," *Dyn. Stab. Syst.,* **4,** 227–243, 1990.
20. C. A. Desoer and M. Vidyasagar, *Feedback Systems: Input-Output Properties,* Academic Press, New York, 1975.
21. M. Vidyasagar, *Nonlinear Systems Analysis,* 2nd ed., Prentice-Hall, Englewood Cliffs, NJ, 1993.
22. J. LaSalle and Z. Artstein, "The stability of dynamical systems," *SIAM Regional Conference Series in Applied Mathematics,* **25,** SIAM, Philadelphia, 1976.
23. G. Niemeyer and J.-J. E. Slotine, "Performance in adaptive manipulator control," *Int. J. Rob. Res.,* **10**(2), 149–161, 1991.
24. T. Fossen, "Comments on 'Hamiltonian adaptive control of spacecraft'," *IEEE Trans. Autom. Control,* **38**(4), 871–872, 1993.
25. F. Miyazaki and S. Arimoto, "Sensory feedback for robot manipulators," *J. Robotic Syst.,* **2**(1), 53–71, 1985.
26. C. J. Damaren and I. Sharf, "Simulation of flexible-link manipulators with inertial and geometric nonlinearities," *ASME J. Dynamic Systems, Measurement, and Control,* **117,** 74–87, 1995.